

Full Length Article

Super-adiabatic temperature in homogenous ignition of CH₄/O₂/N₂ mixtures

Yan Wang, Xinyi Chen, Zheng Chen*

SKLTCs, CAPT, Department of Mechanics and Engineering Science, College of Engineering, Peking University, Beijing 100871, China



ARTICLE INFO

Keywords:

Super-adiabatic temperature
Homogeneous ignition
Premixed flame
Methane

ABSTRACT

Methane-oxygen burning has promising application in future rocket engines used in low-cost space launch systems. In this study, the phenomenon of super-adiabatic temperature (SAT) in homogenous ignition process of methane-oxygen with and without nitrogen dilution is investigated. Simulations considering detailed chemistry are conducted for homogeneous ignition processes and premixed flames in CH₄/O₂/N₂ mixtures. The objectives are to assess the effects of equivalence ratio, oxygen content in oxidizer, initial temperature and pressure on SAT and to identify the key elementary reactions involved in SAT for methane. It is found that the SAT changes non-monotonically with the equivalence ratio and there exists two regimes for SAT. The contribution of each elementary reaction to the post-ignition temperature decrement is quantified and the key reactions responsible for the occurrence of SAT are determined. It is found that the SAT in the homogenous ignition of CH₄/O₂/N₂ mixtures is mainly caused by the endothermic dissociation reactions of H₂O, H₂, CO₂ after thermal runaway. With the increase of initial temperature and oxygen content and decrease of pressure, the dissociation of H₂O, H₂ and CO₂ becomes stronger and thereby SAT is larger. Moreover, the chemistry involved in the SAT for homogeneous ignition and premixed flames is compared. It is found that the same chemical kinetics is involved in the SAT for homogenous ignition process and premixed flames.

1. Introduction

Super-adiabatic temperature (SAT) is a phenomenon in which the maximum combustion temperature is higher than the adiabatic equilibrium temperature. SAT was first observed by Meeks et al. [1] in premixed C₂H₂/H₂/O₂ flames and was attributed to the acetylene dissociation which absorbs heat downstream of the flame front. Another explanation on SAT was proposed by Bertagnolli et al. [2] who suggested that the endothermic dissociation reactions of CO₂ and H₂O in the burned gas induce SAT.

In order to interpret the underlying mechanisms of SAT, extensive studies have been conducted on flame structures of different fuel/air mixtures within a wide range of equivalence ratio. Liu et al. [3] performed systematic numerical analysis on the flame structures of CH₄/air, CH₄/O₂, C₂H₂/H₂/O₂, C₂H₄/O₂, C₃H₈/O₂ and H₂/O₂ mixtures. They found that SAT occurs only in fuel-rich hydrocarbon flames and concluded that complicated chemical kinetics are involved in SAT. Zamashchikov et al. [4] studied the fuel-rich CH₄/air and C₃H₈/air flames and proposed that SAT is caused by the preferential diffusion and

oxidation of H₂ from the reaction zone to the preheating zone. On the contrary, Liu and Gülder [5] demonstrated that SAT is caused by chemical kinetics rather than preferential diffusion of H₂ in fuel-rich CH₄/air and CH₄/O₂ flames. In their numerical study on fuel-rich C₃H₈/air flames, Bunev and Babkin [6] proposed that both chemical kinetics and preferential diffusion of H radical affect the occurrence of SAT.

Furthermore, several studies were conducted to assess the effects of initial temperature, pressure and mixture composition on SAT in premixed flames. Liu and Gülder et al. [7] examined the effects of preheating and pressure increment on fuel-rich CH₄/air flames. They found that preheating inhibits SAT, while increasing pressure enhances SAT. Stelzner et al. [8] investigated SAT in premixed flames of CH₄/O₂/N₂ mixtures with different equivalence ratios and oxygen contents in the oxidizer. They identified two regimes for the appearance of SAT and investigated in-detail the chemical kinetics involved in these two regimes.

Besides premixed flames, SAT was also observed in the homogeneous ignition process for different hydrocarbon fuels. Bunev and Babkin [9]

* Corresponding author.

E-mail address: cz@pku.edu.cn (Z. Chen).<https://doi.org/10.1016/j.fuel.2022.123854>

Received 29 January 2022; Received in revised form 24 February 2022; Accepted 10 March 2022

0016-2361/© 2022 Elsevier Ltd. All rights reserved.

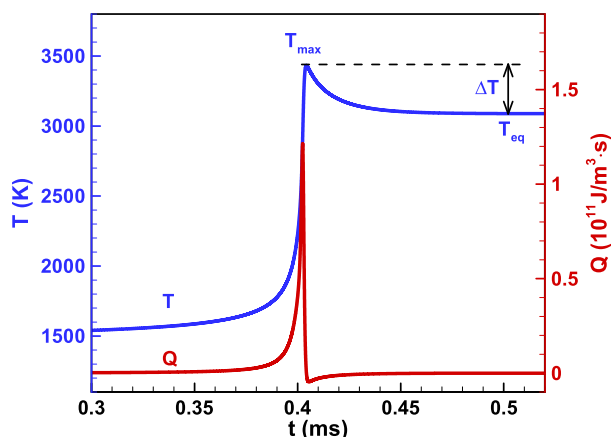


Fig. 1. Evolution of temperature and heat release rate during the homogeneous ignition in a CH_4/O_2 mixture with $\phi = 1.75$, $T_0 = 1500$ K and $P = 1$ atm.

found that the SAT occurring in the homogeneous ignition of dimethyl ether/air mixtures is caused by the competition of the elementary chemical reactions [10]. Recently, the SAT phenomenon in almost stoichiometric and rich methanol/air mixtures has been investigated in detail by S. Rabbani et al. [11]. It was found that with increasing values of equivalence ratio, the explosive character of the ignition process is dominated by endothermic dissociation reactions of carbon-containing species and thereby SAT becomes more pronounced. Compared to premixed flames, the homogeneous ignition process does not involve the convection and diffusion of species and heat. Therefore, SAT in homogeneous ignition process is controlled only by chemical kinetics. Consequently, the key reactions involved in SAT can be identified by studying the homogeneous ignition process. Currently, the chemical kinetics involved in SAT for different hydrocarbon fuels is still not well understood, which motivates the present study.

The objectives of this study are three-folds: (1) to assess the effects of equivalence ratio, oxygen content in oxidizer, and initial temperature and pressure on SAT in homogeneous ignition of $\text{CH}_4/\text{O}_2/\text{N}_2$ mixtures, (2) to identify the key elementary reactions involved in SAT for methane, and (3) to reveal the difference in SAT of homogeneous ignition and premixed flames of $\text{CH}_4/\text{O}_2/\text{N}_2$ mixtures. Currently, methane-oxygen burning is considered for many future rocket engines used in low-cost space launch systems [12]. Besides, compared to other hydrocarbon fuels, methane has well-developed and compact kinetic mechanisms [13,14]. Therefore, CH_4/O_2 mixtures are considered in this study.

2. Numerical model and methods

We simulate the isobaric homogeneous ignition process in $\text{CH}_4/\text{O}_2/\text{N}_2$ mixtures. The mixture composition is determined by the molar ratio of $\text{CH}_4:\text{O}_2:\text{N}_2 = 0.5\phi b:b:(1-b)$, in which ϕ is the equivalence ratio and b is the oxygen volume fraction in the oxidizer. The oxidizer is pure oxygen if $b = 1$. Broad ranges of equivalence ratio, $0.5 \leq \phi \leq 4.0$, and oxygen content in the oxidizer, $0.3 \leq b \leq 1$, are considered. The initial temperature is the range of $1200 \leq T_0 \leq 2000$ K and that for pressure is $0.1 \leq P \leq 10$ atm. In order to compare the SAT appearing in homogeneous ignition process and premixed flames, we also consider one-dimensional, planar, premixed flames in the same $\text{CH}_4/\text{O}_2/\text{N}_2$ mixtures. Both the homogeneous ignition process and premixed flames are simulated using Cantera [15].

Different chemical mechanisms have been developed for methane (see [13,14] and references therein). Since the pressure considered here is no more than 10 atm, GRI-Mech 3.0 [16] consisting of 53 species and 325 elementary reactions is used. In order to demonstrate that the present results are independent of the chemical mechanism used in simulations, we also use one of recent developed mechanisms, FFCM-1

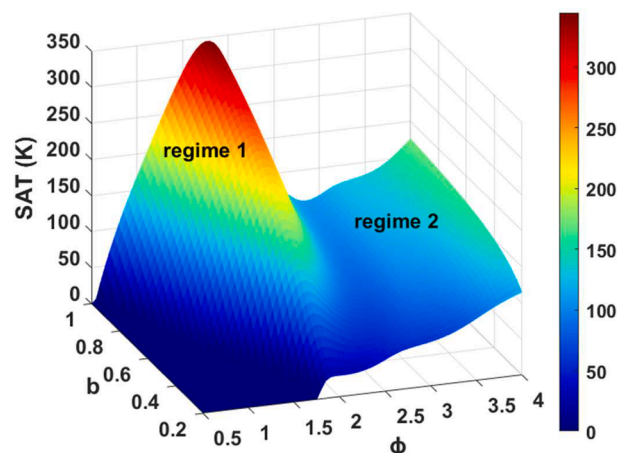


Fig. 2. Change of the super-adiabatic temperature with the oxygen content and the equivalence ratio in homogeneous ignition of $\text{CH}_4/\text{O}_2/\text{N}_2$ mixtures at $T_0 = 1500$ K and $P = 1$ atm.

[17], and the results from GRI-Mech. 3.0 and FFCM-1 are briefly compared.

3. Results and discussion

3.1. Super-adiabatic temperature

Fig. 1 shows the evolution of temperature and heat release rate during the homogeneous ignition of a fuel-rich CH_4/O_2 mixture. Immediately after thermal runaway (i.e. autoignition), the temperature reaches its maximum value of $T_{max} = 3433$ K and then it starts to decrease due to the negative heat release rate in the post-ignition regime. Eventually, the equilibrium temperature of $T_{eq} = 3088$ K can be reached. The maximum temperature is much higher than the equilibrium temperature. Their difference, $\Delta T = T_{max} - T_{eq} = 345$ K is referred to as the super-adiabatic temperature (SAT). In numerical simulations, the simulation time is long enough to make sure that a constant value for equilibrium state is reached for T_{eq} .

Fig. 2 shows the change of the super-adiabatic temperature, $\text{SAT} = \Delta T = T_{max} - T_{eq}$, with the equivalence ratio, ϕ , and the oxygen content, b . It is observed that the super-adiabatic temperature changes non-monotonically with the equivalence ratio, and reaches its peak value around $\phi = 1.75$. There are two regimes for the super-adiabatic

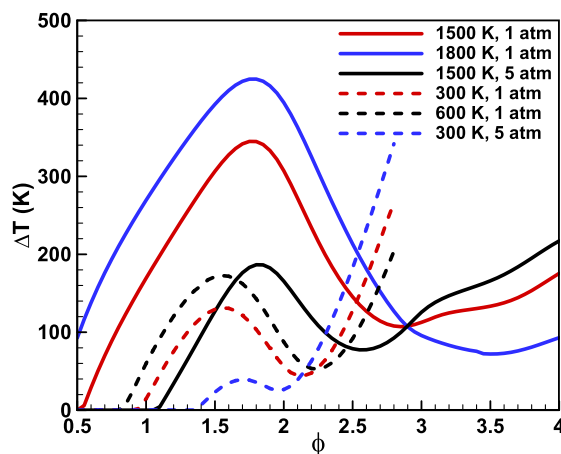


Fig. 3. Change of the super-adiabatic temperature with equivalence ratio for homogeneous ignition (solid lines) and premixed flames (dashed lines) in CH_4/O_2 mixtures at different initial temperatures and pressures.

temperature. The first regime occurs at moderately fuel-rich condition with $\phi < 2.5$ and relatively high oxygen content; while the second regime occurs at very fuel-rich side with $\phi > 2.5$ and over the full range of oxygen content. The SAT increases substantially with the oxygen content in the first region, whereas it is insensitive to the oxygen content in the second regime. As oxygen content decreases, the first regime gradually disappears. Therefore, SAT strongly depends on both the equivalence ratio and oxygen content. Note that two regimes for the appearance of SAT were also found for premixed $\text{CH}_4/\text{O}_2/\text{N}_2$ flames by Stelzner et al. [8]. Fig. 2 shows that for autoignition, the maximum SAT in regime 1 is much larger than that in regime 2. However, for premixed flames the maximum SAT in regime 1 is much smaller than that in regime 2 (see Fig. 3 in [8]). This indicates that SAT in autoignition is induced by different factors from that in premixed flames.

To demonstrate that the two SAT regimes occurs for different initial temperatures and pressures, we consider CH_4/O_2 mixtures without nitrogen (i.e., $b = 1$). Fig. 3 shows the results for three sets of initial temperature and pressure: (1500 K, 1 atm), (1800 K, 1 atm) and (1500 K, 5 atm). It is seen that two regimes always appear. Comparison between the red and blue solid lines in Fig. 3 shows that increasing the initial temperature from 1500 K to 1800 K enhances SAT in the first regime while reduces SAT in the second regime. On the contrary, increasing the pressure from 1 atm to 5 atm reduces SAT in the first regime but enhances SAT in the second regime. Similar trends are observed for SAT in premixed flames, as shown by the dashed lines in Fig. 3. The turning point is caused by the change of chemical kinetics in the two SAT regimes [8]. With relatively high oxygen concentration in the first regime, the kinetics is very fast and locally almost in equilibrium. Therefore, this regime is dominated by the high temperature oxidation pathways (formaldehyde \rightarrow formyl \rightarrow carbon monoxide). When the equivalence ratio increases, C_2 -pathway-reactions with the absence of oxygen become the dominant reactions in the second regime. Fig. 3 also shows that unlike premixed flames, homogenous ignition process has relatively larger SAT in the first regime and relatively smaller SAT in the second regime. This is due to the facts that the initial temperature for homogenous ignition, 1500 or 1800 K, is much higher than 300 or 600 K for premixed flames, and that increasing the initial temperature enhances (reduces) SAT in the first (second) regime.

The above results demonstrate that two SAT regimes are observed in both homogeneous ignition process and premixed flames. The equivalence ratio in the second regime is very high and it is beyond the scope of the typical operating conditions. Therefore, in the following subsections, the chemical kinetics related to the SAT in the first regime is discussed in-detail.

3.2. Chemical reactions involved in SAT

We choose a reference case with $\phi = 1.75$, $b = 1$, $T_0 = 1500$ K and $P = 1$ atm for which the super-adiabatic temperature is $\Delta T = 345$ K. In the following, the key elementary reactions involved in the SAT phenomenon are identified for different initial temperatures, pressures, and oxygen contents in the oxidizer.

In order to quantify the contribution of different elementary reactions to SAT, the temperature decrease caused by the k -th reaction is evaluated as:

$$\Delta T_k = - \int_{t_{\max}}^{t_{eq}} \frac{\dot{q}_k}{\rho C_p} dt \quad (1)$$

where \dot{q}_k is the heat release rate from the k -th reaction, ρ the density, and C_p the specific heat capacity of the mixture. In Eq. (1), t_{\max} is the instant when the temperature reaches its maximum value and t_{eq} is the instant when the equilibrium temperature is reached. The negative sign indicates positive contribution of endothermic reaction to SAT.

Based on the analysis of the contribution of each elementary reaction to SAT, we identify the following reactions which mainly induce SAT:

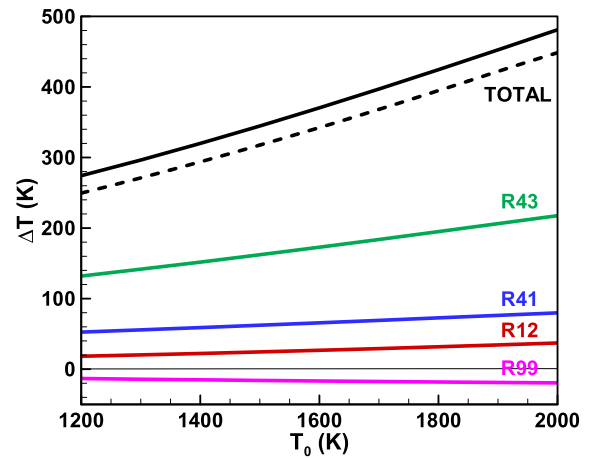


Fig. 4. Change of the contribution of main reactions to the super-adiabatic temperature with initial temperature for the homogeneous ignition in a CH_4/O_2 mixture with $\phi = 1.75$ and $P = 1$ atm. The solid lines represent results predicted by GRI-Mech 3.0 while the dash line is from FFCM-1.

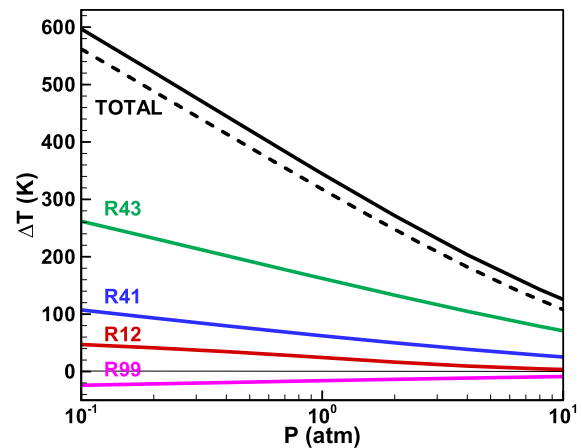


Fig. 5. Change of the contribution of main reactions to the super-adiabatic temperature with pressure for the homogeneous ignition in a CH_4/O_2 mixture with $\phi = 1.75$ and $T_0 = 1500$ K. The solid lines represent results predicted by GRI-Mech 3.0 while the dash line is from FFCM-1.



Fig. 4 shows that SAT is mainly caused by the dissociation of H_2O , H_2 and CO_2 through reactions R43, R41 and R12, respectively. Compared to R43 and R41, the dissociation of CO_2 by R12 has a relatively smaller contribution. Reaction R99 is exothermic and thereby contributes negatively to SAT. Similar conclusions are obtained through FFCM-1, where the dissociation of H_2O , H_2 , CO_2 are responsible for the occurrence of SAT. However, the relative importance of the endothermic reactions varies in different mechanisms. Besides, Fig. 4 shows that with the increase of the initial temperature, there is stronger dissociation of H_2O . This is consistent with the Le Chatelier's principle that the endothermic reaction is enhanced at higher temperature. Consequently, SAT increases with the initial temperature. Note that Fig. 4 shows results from GRI-Mech 3.0 and FFCM-1 are very close, indicating that the

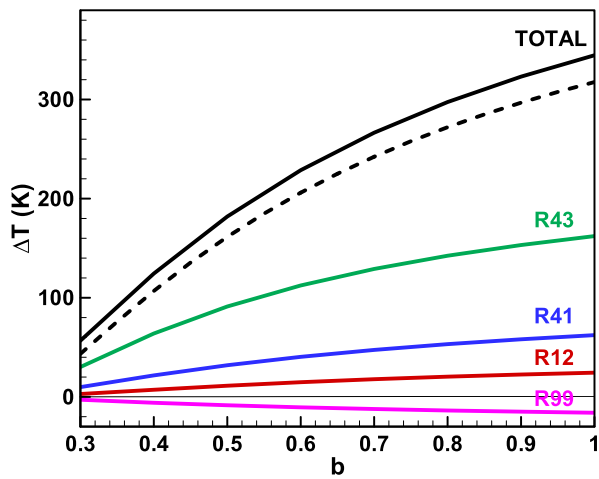


Fig. 6. Change of the contribution of main reactions to the super-adiabatic temperature with oxygen content for the homogeneous ignition in a $\text{CH}_4/\text{O}_2/\text{N}_2$ mixture with $\phi = 1.75$, $T_0 = 1500$ K and $P = 1$ atm. The solid lines represent results predicted by GRI-Mech 3.0 while the dash line is from FFCM-1.

present conclusions are independent of the chemical mechanism used in simulations.

Fig. 5 shows the results at different pressures. It is seen that at both sub-atmospheric and elevated pressures, SAT is also mainly caused by the dissociation of H_2O , H_2 and CO_2 through reactions R43, R41 and

R12. With the increase of pressure, the dissociation of H_2O , H_2 and CO_2 is suppressed according to Le Chatelier's principle. Therefore, SAT is shown to decrease with the pressure. Again, Fig. 5 shows that the present results are independent of the chemical mechanism used in simulations.

Similar to the initial temperature, the oxygen content in oxidizer also affects the maximum combustion temperature and thereby affects the dissociation of H_2O , H_2 and CO_2 after thermal-runaway. With the increase of oxygen content, the maximum temperature is higher and thereby the endothermic dissociation of H_2O , H_2 and CO_2 becomes stronger. Consequently, Fig. 6 shows that SAT increases with the oxygen content and that SAT is mainly caused by reactions R43, R41 and R12.

In a brief summary, SAT in the homogeneous ignition of $\text{CH}_4/\text{O}_2/\text{N}_2$ mixtures is mainly caused by the dissociation of H_2O , H_2 and CO_2 through reactions R43, R41 and R12. With the increase of initial temperature and oxygen content and decrease of pressure, the dissociation of H_2O , H_2 and CO_2 becomes stronger and thereby SAT is larger. Similar effects of initial temperature, pressure and oxygen content on the SAT were also observed for premixed flames in previous study [8].

3.3. Comparison SAT in homogeneous ignition and premixed flames

The above two sub-sections demonstrate that SAT is mainly induced by the endothermic dissociation reactions R43 ($\text{H}_2\text{O} + \text{M} = \text{H} + \text{OH} + \text{M}$) and R41 ($\text{H}_2 + \text{H}_2\text{O} = 2\text{H} + \text{H}_2\text{O}$). As the species involved into these two reactions, H and H_2O have great impact on the chemical equilibrium of these two reactions and the value of SAT. Therefore, in this subsection, the chemical pathway for H and H_2O production in homogeneous ignition is examined and is compared with that in premixed flames.

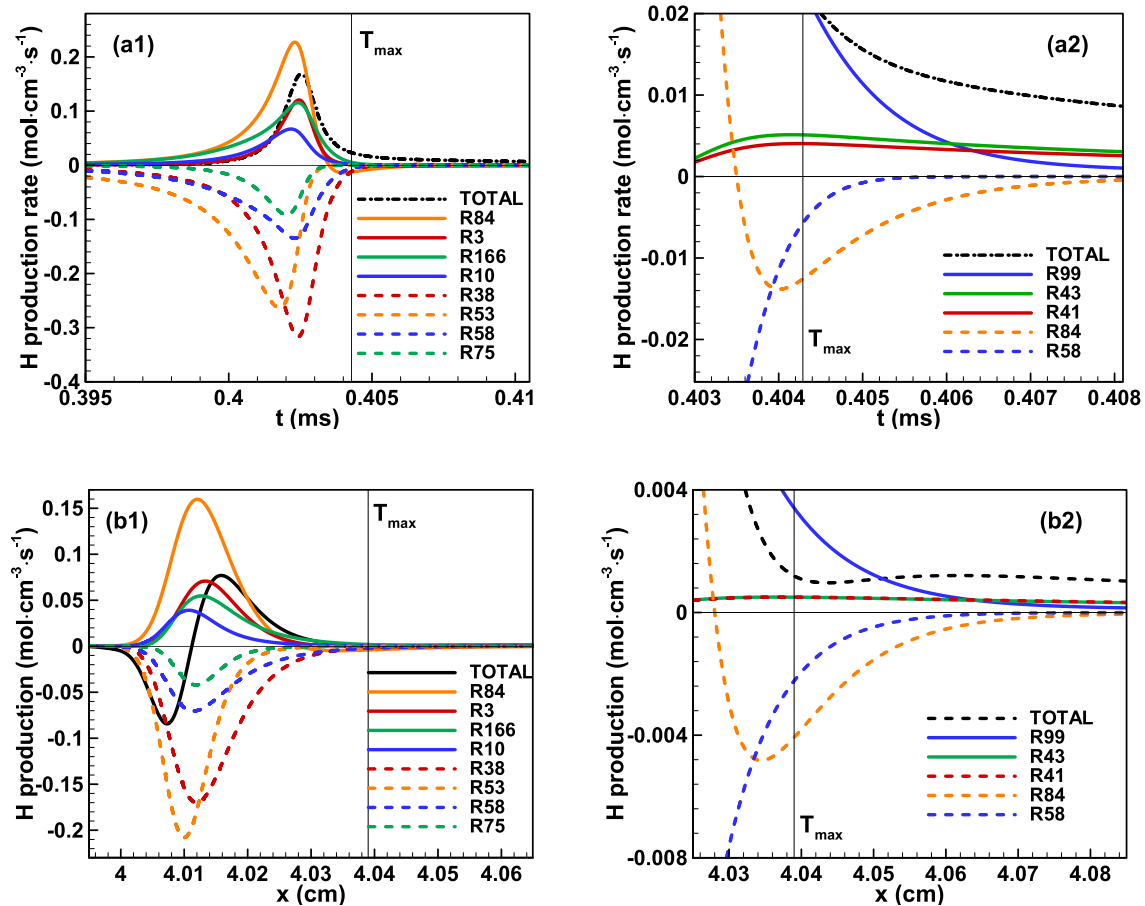


Fig. 7. Production rates of H radical by difference elementary reactions in: (a1) and (a2), homogeneous ignition of CH_4/O_2 mixture with $\phi = 1.75$, $T_0 = 1500$ K and $P = 1$ atm; and (b1) and (b2) premixed flame of CH_4/O_2 mixture with $\phi = 1.75$, $T_0 = 300$ K and $P = 1$ atm. The vertical black line represents the time or position for the appearance of maximum temperature.

Table 1
Reactions producing and consuming H radical.

Reactions producing H	Reactions consuming H
R84: $\text{OH} + \text{H}_2 = \text{H} + \text{H}_2\text{O}$	R38: $\text{H} + \text{O}_2 = \text{O} + \text{OH}$
R3: $\text{O} + \text{H}_2 = \text{H} + \text{OH}$	R53: $\text{H} + \text{CH}_4 = \text{CH}_3 + \text{H}_2$
R10: $\text{O} + \text{CH}_3 = \text{H} + \text{CH}_2\text{O}$	R58: $\text{H} + \text{CH}_2\text{O} = \text{HCO} + \text{H}_2$
R166: $\text{HCO} + \text{H}_2\text{O} = \text{H} + \text{CO} + \text{H}_2\text{O}$	R75: $\text{H} + \text{C}_2\text{H}_4 = \text{C}_2\text{H}_3 + \text{H}_2$

Fig. 7 shows the production rate of H radical by difference elementary reactions for CH_4/O_2 mixture with $\phi = 1.75$. It is seen that the H radical is mainly generated by R84, while consumed by R38, R53 in both homogeneous ignition and premixed flame. These dominant reactions are listed in Table 1 and are consistent with the study of Stelzner et al. [8].

Although the dominant reactions are the same in both two homogeneous ignition and premixed flame, discrepancy is observed in the H production profiles. This is mainly caused by the fact that unlike premixed flame, there is no H radical transportation in homogeneous ignition process. Therefore, the total H production rate is positive over the whole homogenous ignition process. However, in the premixed flame, the total H production rate is negative in the preheat zone and positive in the reaction zone. Regarding to the H production rates by elementary reactions, Fig. 7 shows that reaction R166 is enhanced without H diffusion loss, while reaction R53 is weakened without H diffusion supplement. After the appearance of maximum temperature, T_{\max} , H radical is mainly generated by reactions R43, R41 and R99.

Fig. 8 shows the production rate of H_2O by difference elementary

reactions. It is observed that H_2O is mainly generated from R84 and R98, and then R96, R97, R101 in both homogeneous ignition and premixed flame. These dominant reactions are listed in Table 2 and are consistent with the study of Stelzner et al. [8]. Through these reactions, the super equilibrium concentration of H_2O is reached just after the main heat release.

The negative production rate for H_2O after appearance of maximum temperature, T_{\max} , is further shown in Fig. 8(a2) and (b2). It is observed that the negative production rate for H_2O is first dominated by reversed reaction -R84 and then by reaction R43 until the mixture reaches the equilibrium state. It is noted that with no H radical transportation to upstream in homogeneous ignition, less H_2O are produced in the reaction zone. As a consequence, the dissociation of H_2O is suppressed and the SAT is decreased. As shown before, the H_2O dissociation reaction R43 is the key reaction inducing the SAT phenomenon. Therefore, the same chemical kinetics is involved in the SAT for homogenous ignition process and premixed flames.

Table 2
Reactions producing and consuming H_2O radical.

Reactions producing H_2O	Reactions consuming H_2O
R84: $\text{OH} + \text{H}_2 = \text{H} + \text{H}_2\text{O}$	R84: $\text{H} + \text{H}_2\text{O} = \text{OH} + \text{H}_2$
R98: $\text{OH} + \text{CH}_4 = \text{CH}_3 + \text{H}_2\text{O}$	R43: $\text{H}_2\text{O} + \text{M} = \text{H} + \text{OH} + \text{M}$
R96: $\text{OH} + \text{CH}_3 = \text{CH}_2 + \text{H}_2\text{O}$	
R97: $\text{OH} + \text{CH}_3 = \text{CH}_2(\text{S}) + \text{H}_2\text{O}$	
R101: $\text{OH} + \text{CH}_2\text{O} = \text{HCO} + \text{H}_2\text{O}$	

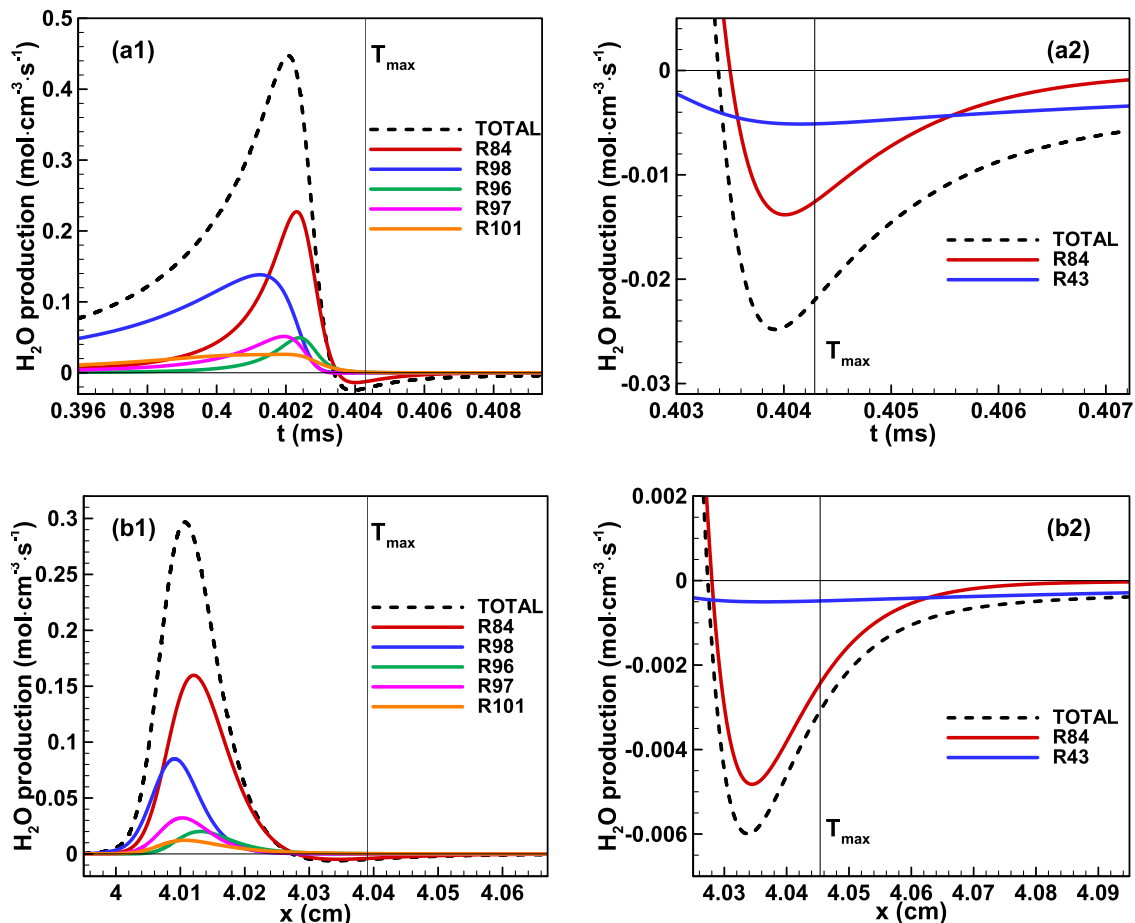


Fig. 8. Production rates of H_2O by difference elementary reactions in: (a1) and (a2), homogeneous ignition of CH_4/O_2 mixture with $\phi = 1.75$, $T_0 = 1500$ K and $P = 1$ atm; and (b1) and (b2) premixed flame of CH_4/O_2 mixture with $\phi = 1.75$, $T_0 = 300$ K and $P = 1$ atm. The vertical black line represents the time or position for the appearance of maximum temperature.

4. Conclusions

Transient simulations considering detailed chemistry are conducted to investigate the super-adiabatic temperature (SAT) phenomenon in homogenous ignition process. The CH₄/O₂/N₂ mixtures with a broad range of equivalence ratio and oxygen content at different initial temperatures and pressures are considered. Two regimes of SAT are observed: the first regime occurs at moderately fuel-rich condition with $\phi < 2.5$ and relatively high oxygen content; while the second regime occurs at very fuel-rich side with $\phi > 2.5$ and over the full range of oxygen content. It is found that SAT increases substantially with the oxygen content in the first region, whereas it is insensitive to the oxygen content in the second regime. Similar trends are observed for SAT in premixed flames. However, homogenous ignition process has relatively larger SAT in the first regime and relatively smaller SAT in the second regime; while the opposite hold for SAT in premixed flames. This is mainly due to the very large difference in initial temperatures for homogenous ignition and premixed flames. The SAT in the homogenous ignition of CH₄/O₂/N₂ mixtures is found to be mainly caused by the dissociation reactions of H₂O, H₂ and CO₂. With the increase of initial temperature and oxygen content and the decrease of pressure, the dissociation of H₂O, H₂ and CO₂ becomes stronger and thereby SAT is larger. Besides, the chemical pathways of H and H₂O production in homogenous ignition are examined and compared with those in premixed flames. It is found that the dominant reactions of H and H₂O production are the same in both two configurations. Besides, since there is no H radical transportation in homogeneous ignition, less H₂O is produced in the reaction zone of homogeneous ignition process that that in premixed flames. Consequently, the dissociation of H₂O is suppressed and the SAT is reduced. The difference in the production rate profiles for H and H₂O is mainly due to the mass diffusion in premixed flames.

CRediT authorship contribution statement

Yan Wang: Conceptualization, Writing – original draft. **Xinyi Chen:** Supervision, Writing – review & editing. **Zheng Chen:** Conceptualization, Supervision, Writing – review & editing, Project administration, Funding acquisition.

Declaration of Competing Interest

The authors declare that they have no known competing financial interests or personal relationships that could have appeared to influence the work reported in this paper.

Acknowledgement

This work was supported by National Natural Science Foundation of China (No. 52176096).

References

- [1] Meeks E, Kee RJ, Dandy DS, Coltrin ME. Computational simulation of diamond chemical vapor deposition in premixed C₂H₂/O₂/H₂ and CH₄/O₂-strained flames. *Combust Flame* 1993;92:144–60.
- [2] Bertagnolli KE, Lucht RP, Bui-Pham MN. Atomic hydrogen concentration profile measurements in stagnation-flow diamond-forming flames using three-photon excitation laser-induced fluorescence. *J Appl Phys* 1998;83(4):2315–26.
- [3] Liu F, Guo H, Smallwood GJ, Gülder ÖL. Numerical study of the superadiabatic flame temperature phenomenon in hydrocarbon premixed flames. *Proc Combust Inst* 2002;29(2):1543–50.
- [4] Zamashchikov VV, Namyatov IG, Bunev VA, Babkin VS. On the nature of superadiabatic temperatures in premixed rich hydrocarbon flames. *Combust Explos Shock Waves* 2004;40(1):32–5.
- [5] Liu F, Gülder ÖL. Effects of H₂ and H preferential diffusion and unity Lewis number on superadiabatic flame temperatures in rich premixed methane flames. *Combust Flame* 2005;143(3):264–81.
- [6] Bunev VA, Babkin VS. Chemical reactions in the low-temperature zone of a laminar rich propane–air flame. *Combust Explos Shock Waves* 2006;42(5):503–8.
- [7] Liu F, Gülder ÖL. Effects of pressure and preheat on super-adiabatic flame temperatures in rich premixed methane/air flames. *Combust Sci Technol* 2008;180(3):437–52.
- [8] Stelzner B, Weis C, Habisreuther P, Zarzalis N, Trimis D. Super-adiabatic flame temperatures in premixed methane flames: A comparison between oxy-fuel and conventional air combustion. *Fuel* 2017;201:148–55.
- [9] Bunev VA, Babkin VS. Effect of superadiabatic temperatures in the autoignition of dimethyl ether mixtures. *Mendeleev Commun* 2009;19(5):290–1.
- [10] Babkin VS, Bunev VA, Bolshova TA. Superadiabatic temperature phenomenon in the combustion processes due to a competition between chemical reactions. *Combust Explos Shock Waves* 2015;51(2):151–9.
- [11] Rabbani S, Manias DM, Kyritsis DC, Goussis DA. Chemical dynamics of the autoignition of near-stoichiometric and rich methanol/air mixtures. *Combust Theor Model* 2021:1–31.
- [12] Neill T, Judd D, Veith E, Rousar D. Practical uses of liquid methane in rocket engine applications. *Acta Astronaut* 2009;65(5-6):696–705.
- [13] Zhang IGZP, Papp M, Nagy T, Turányi T. Comparison of methane combustion mechanisms using laminar burning velocity measurements. *Combust Flame* 2022; 238:111867.
- [14] Wang Y, Movaghar A, Wang Z, Liu Z, Chen Z. Laminar flame speeds of methane/air mixtures at engine conditions: Performance of different kinetic models and power-law correlations. *Combust Flame* 2020;218:101–8.
- [15] Goodwin DG, Moffat HK, Speth RL. Cantera: An object-oriented software toolkit for chemical kinetics, thermodynamics, and transport processes. version 2.3.0. <https://zenodo.org/record/170284>; 2017.
- [16] Wu Yi, Modica V, Rossow B, Grisch F. Effects of pressure and preheating temperature on the laminar flame speed of methane/air and acetone/air mixtures. *Fuel* 2016;185:577–88.
- [17] Smith YTGP, Wang H. Foundational fuel chemistry model version 1.0 (FFCM-1). <http://nanoenergy.stanford.edu/ffcm1>; 2016.